Mass-Transfer Parameters in Gas-Solid Reactive Media to Identify Permeability of IMPEX

Hui-Bo Lu and Nathalie Mazet
CNRS-Institut de Science et de Génie des Matériaux et Procédés, Laboratoire Européen Associé SIMAP, 66860 Perpignan-Cedex, France

Lu et al.'s modeling of gas-solid reaction demonstrated the significant influence of mass transfer on the global transformation of consolidated porous reactive media with reactive gas at low pressure and low permeability. Their model coupled mass transfer with chemical kinetics at the grain level and heat transfer with mass transfer at the pellet level. The comparison between simulation results and recent experiments demonstrated that the value of the material permeability varies during the reaction process. This study presents the permeability decrease during the synthesis process. A correlation representing the nonlinear evolution of permeability was identified for different reactive materials used for experiments. These mechanisms can satisfactorily explain both the experimental measurements of global advancement and local temperature profiles.

Introduction

Thermochemical processes that involve monovariant reversible reaction of ammonia and metal chlorides have been under full development since the beginning of the 1980s. These processes of solid-gas reactions present an important perspective for the rational use of energy and as a response to environmental concerns (Spinner, 1988, 1993). Moreover, they have opened a spectrum of new technical applications (Spinner, 1996; Satzger et al., 1996), including storage of heat and cold generation with instant high-capacity power output and self-managed system by means of specific properties of the material used.

The development and the improved performance of these systems depend strongly on the material pre-conditioned treatment. This can be achieved by means of a deep understanding and evaluation of the proper heat- and mass-transfer characteristics of the system as a whole. In this article, we present our continued study on the combined influences of heat and mass transfer on the global transformation of such solid-gas media. Their limitations are presented in a Clausius-Clapeyron diagram (Figure 1): a solid-gas reaction can only take place when the out-of-equilibrium constraints P_C, T_C are imposed on the reactive media. These constraints are generally applied on the two extreme geometric ends of the reactor, while inside the reactor, local conditions $P(r)$, $T(r)$ move towards the equilibrium according to the trajectory indicated in Figure 1.

Two methods have been taken to improve the overall performance of the porous reactive material. These are:

- Heat-transfer enhancement through an increase of main heat-transfer parameters, that is, the equivalent conductivity of the reactive block and contact heat-transfer coefficient between the reactive block and the heat exchanger.
- Mass-transfer enhancement by means of an increase of main mass-transfer parameters, that is, permeability in the reactive block.

In reply to such demands, a novel processing of composite blocks has been developed: the IMPEX Material, patented by Le Carbone Lorraine (Coste et al., 1986; Mauran et al., 1991).

IMPEX shows significant improvements on heat-transfer characteristics, due to its graphite matrix (Mauran et al., 1991, 1993; Guilleminot, 1993). The main heat-transfer limitation for IMPEX remains the contact heat-transfer coefficient (h_{sw}) (W/m^2K) at the reactor wall: it depends on the density of the

Correspondence concerning this article should be addressed to N. Mazet.
Current address of H.-B. Lu: Hui Bo Technologies (Shanghai) Co. Ltd., Building No 1, 2019 Jiang Chuan Road, Ming Hang, District, 200240, Shanghai, P.R. China.

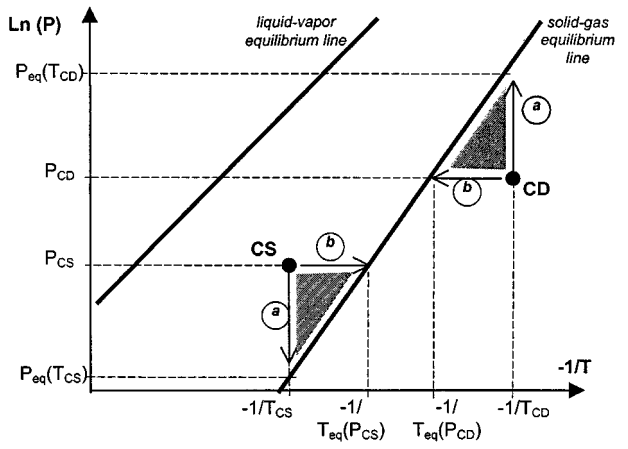

Figure 1. Typical effect of transfer limitations in a Clausius-Clapeyron diagram.

●, Thermodynamic constraints during synthesis (CS) and decomposition (CD); →, evolution of local working conditions for (a) strong mass-transfer limitation, (b) strong-heat transfer limitation.

material used and on the contact conditions between the reactive block and the heat exchanger. The study of Castaing-Lasvignottes and Spinner (1994) has shown that h_{sw} of IMPEX block has a nonlinear evolution during the reaction process. In the onset of the synthesis, the salts quickly absorb the reactive gas and the block tends to expand. This results in a better contact between the block and heat exchanger. Then, during the process of decomposition, the reactive block detaches from the heat exchanger when gas is released and h_{sw} decreases.

On the other hand, mass-transfer limitation in a reactive block has progressed recently. Lu et al. (1996) has developed a general model which couples mass transfer with chemical kinetics at the grain level, and heat with mass transfer at the pellet level. This model has quantitatively underscored the theoretical scope of mass-transfer influence on the reaction, whose two major parameters are operating pressure and permeability. Comparison between simulations and measurements has revealed that permeability varies during the reaction. During synthesis reaction, the density of the reactive block increases and the gas passage narrows. At a certain stage, the gas passage is nearly blocked. This results in a sharp decrease of permeability at that position. Inversely, during the decomposition process, the reactive block structure becomes more porous, leading to an increase in permeability.

Studies of the variation of the permeability of the material during the process of reversible gas-solid reaction are very rare in the literature. One can find related approach, however, for gas flowing processes in porous nonreactive media, as the one encountered in the analysis of gradual flow blocking in gas/oil rocks penetration (Wojtanowicz, 1988).

Therefore, the objective of this article is to study the mechanism of the evolution of the material permeability during a chemical reaction process in order to evaluate the sensitivities of the various parameters involved, their influences on the global advancement of the reaction, and their local profiles within the material. The simulation results have been widely compared with recent experimental findings.

Diffusions of Heat and Mass Coupled with Chemical Reaction

Modeling

The porous reactive media used in thermochemical transformers are characterized by a strong coupling between reactive gas diffusion, heat transfer in the solid matrix, and the chemical reaction (Mazet et al., 1991). The detailed modeling of such coupling can be found in Lu et al. (1996). A grain-pellet type model (Szekely et al., 1976; Sun and Meunier, 1987) is used. The principle and basic equations are summarized as follows.

At the Grain Level. To start with, one assumes that the reaction takes place on a sharp reactive front in the grain. At grain level, the temperature is assumed uniform. Mass transfer between the external surface of the grain and the reaction front is described by Darcy's law. Chemical reaction kinetics at the interface depends on the driving force, that is, the equilibrium drop (Goetz and Marty, 1993). A pseudo-steady state is assumed. A balance of mass diffusion and gas flux from the reaction leads to the resulting mass flux at the grain level as a function of external pressure (Pa) and temperature (k) of the grain: P_{grain} and T_{grain}

$$dNg/dt = f\left(P_{\text{grain}}, T_{\text{grain}}\right) \tag{1}$$

where Ng is the number of moles of reactive gas (moles per grain).

At the Cylindrical Pellet Level (Reactor Geometry). Heat and mass transfer are considered in the radial direction, and convective terms are neglected. In each elementary volume, characterized by local values $P(r,t)$ and $T(r,t)$, the local source term is defined by the mass-flow rate generated by the chemical reaction. This volume is supposed to have the similar behavior as a grain submitted to the same pressure and temperature. Therefore, the previous expression of mass flux generated by a single grain can be used in the source term of mass and heat balance at the pellet level

$$I = N_{\text{tot}}\frac{dNg}{dt} = f\left[P, T, x(r)\right] \tag{2}$$

where N_{tot} is the total number of grains in the elementary volume.

Usually, one prefers to replace the number of moles of gas by the local advancement of the reaction defined by the ratio

$$x(r) = Ng(r)/Ng_{\max} \tag{3}$$

where $Ng_{\max}$ is the maximum number of mole of gas fixed on the solid in the representative elementary volume. It depends on the chemical reaction stoichiometry and on the molar density of the solid.

Heat Balance is Described by the Following Equation

$$C_p\left[x(r)\right]\frac{\partial T}{\partial t} = \frac{1}{r}\frac{\partial}{\partial r}\left[r\lambda_e\frac{\partial T}{\partial r}\right] + I\Delta H \tag{4}$$

Mass Balance is Described by the Equation

$$\epsilon_p \frac{\partial P}{\partial t} = \epsilon_p \frac{P}{T}\left(\frac{\partial T}{\partial t}\right) + \frac{RT}{r}\frac{\partial}{\partial r}\left(r\frac{D_p}{RT}\frac{\partial P}{\partial r}\right) - RTI \qquad (5)$$

Experimental results demonstrate that the diffusivity in the pellet (D_p) (m^2/s) depends on the gas pressure, according to Darcy's law

$$D_p = \frac{k_e P}{\mu} \qquad (6)$$

Boundary Conditions

At the heat exchanger wall (r_w), these are expressed as the continuity of the heat flux through the surface

$$\lambda_e \frac{\partial T}{\partial r} = h_{sw}\left[T_c - T(r)\right] \qquad (7)$$

At the mass diffuser side, the pressure is fixed. The other boundary and initial conditions are classical ones (Lu et al., 1996).

The molar volume of the reactive salt is 3 times smaller than that of the reactive product. Consequently, the modeling must take into account a variation of physical parameters during the reaction. The permeability in the pellet k_e and the heat-transfer coefficient at the reactor wall h_{sw} are expressed vs. the local advancement

$$k_e = k\left[x(r)\right] \qquad h_{sw} = h_{sw}\left[x(r_w)\right] \qquad (8)$$

The resolution of these differential equations coupled at grain and pellet levels results in local profiles of advancement, temperature, pressure, and subsequently the global advancement (that is, mean value for the whole reactor).

Permeability evolution

Accurate measurements of permeability can be performed at initial and final states of the reaction, that is, for global advancement equal to 0 or 1. In such a case, the source term associated with the reaction can be neglected and the gas flux is precisely estimated. These two values are called k_0 (at its initial state) and k_1 (at the end of the completed synthesis). Measurements made on IMPEX blocks led to values of k_1 smaller than k_0 by several orders of magnitude. This difference is supposed to be due to the variation of the molar volume and therefore to structural changes within the reactive material.

Experimental results in the reaction process give correlated information: the synthesis reaction presents a significant slowdown at a global advancement lower than 1 (as will be seen in Figure 8). This is much more evident at low pressure. The cause for this sudden slowdown of global transformation is very likely to be a sharp change in permeability value from k_0 to k_1.

From several numerical approaches, a nonlinear correlation of the permeability which characterizes this sharp change of local permeability has been chosen and will be compared with experimental results. For the synthesis reaction, X_S is defined as the inflection point where the sharp drop-off of permeability occurs. Therefore, the permeability as a function of local advancement is expressed as

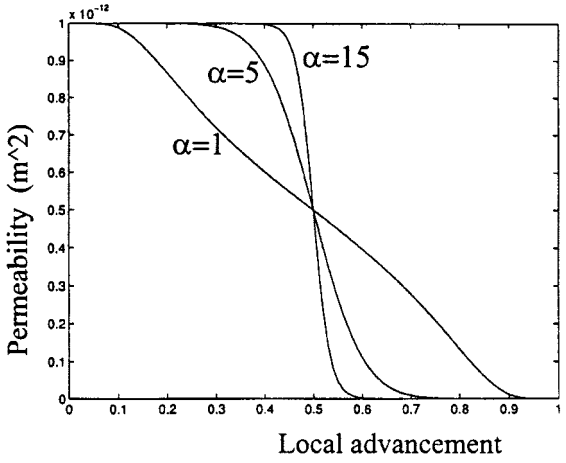

Figure 2. Sensibilities of the nonlinear evolution of permeability ($X_S = 0.5$).

$$k = k_1 + \frac{k_0 - k_1}{1 + \exp\left[\alpha \dfrac{x - X_s}{x(1-x)}\right]} \qquad (9)$$

where x is the local advancement and α is a factor which controls the angular magnitude of the permeability drop-off curve.

Previous works (Lu et al., 1996) have shown that if the permeability of a reactive medium is less than 10^{-16} m^2, the reaction is such a medium is completely blocked. On the other hand, if permeability is higher than 10^{-13} m^2, transformation of the reactive media is close to that encountered in an ideal isobaric condition (no limitation of mass transfer). Between these two cases, the combined influence of heat and mass transfer is evident. Therefore, the range from $k_0 = 10^{-13}$ m^2 to $k_1 = 10^{-16}$ m^2 has been used. Typical behaviors of k as a function of α are presented in Figure 2, within the defined range, and for $X_S = 0.5$. It shows that a sharp permeability drop requires α values equal or superior to 5: this value is then fixed in further simulations. Value of X_S only leads to a shift of curves along x axis in Figure 2.

Therefore, the parameters k_0, k_1 and X_S of Eq. 9 must be identified for each reactive material, and then verified for the same material under different operating conditions.

Influence of permeability evolution on reactor transformation

Our objective is to find out, theoretically, the influence of the nonlinear local evolution of permeability (mainly characterized by X_s) on the reactive block transformation, particularly on local profiles. The selected reactive blocks are within practical application range and are totally realistic. Other physical parameters of reactive blocks are listed in Table 1 (IMPEX 1). Figures 3 and 4 show the influence of different local evolutions of permeability on global transformation, lo-

Table 1. Characteristics of IMPEX Samples

Parameter/No. IMPLEX	Symbol	1	A	B	C	D
Apparent density of graphite binder, kg/m^3	ρ_1	160	200	238	223	228
Mass ratio of graphite binder		30%	46%	60%	43%	37%
Apparent density of IMPLEX, kg/m^3		518	427	398	519	618
Porosity of the pellet						
At the synthesis onset	ϵ_0	0.7	0.76	0.79	0.71	0.65
At the synthesis end	ϵ_1	0.45	0.61	0.69	0.53	0.41
Conductivity of the pellet, W/(m·K)						
At the synthesis onset	λ_0	15	23	18	18	18
At the synthesis end	λ_1	15	32	18	18	18
Heat-transfer coefficient at the pellet/wall contact, W/(m^2·K)						
At the synthesis onset	h_{SW0}	500	150	600	80	40
At the synthesis end	h_{SW1}	500	550	3,000	3,000	3,000
Permeability of the pellet, m^2		Fixed values:				
Identified value: at the synthesis onset	k_0	10^{-13}	5×10^{-13}	4×10^{-12}	10^{-12}	10^{-13}
at the synthesis end	k_1	10^{-16}	10^{-16}	10^{-16}	10^{-16}	10^{-16}
Identified value of X_S, see Eq. 9	X_S	0.0 to 1.0	0.1	0.35	0.3	0.25

cal advancement, and temperature and pressure profiles in the reactor during synthesis process.

The simulation of the global advancements are represented in Figure 3. Simulations using either constant permeability (for extreme values of k, solid lines) or a linear evolution of k in the same range (dash dot line) do not represent the typical sharp slowdown observed in experimental results (Lu et al., 1996; or see an example which will be shown in Figure 6). On the other hand, simulations based on a nonlinear evolution of k as Eq. 9 (in dotted lines, for $X_S = 0.25$, 0.5, 0.75) present the rapid slowdown of the global advancement, which is similar to that obtained by experiments. Based on these arguments, Eq. 9 for $k(x)$ is therefore chosen.

Figure 4 presents a typical simulation of local profiles of advancement, temperature and pressure, during a synthesis reaction. This typical simulation is based on a nonlinear evolution of $k(x)$, characterized by $X_S = 0.5$. On each sub-plot, the different profiles correspond to increasing values of the global advancement (printed near each profile). The X-axis represents the radial position of the reactor, bounded by the gas diffuser ($r = 5$ mm) and the heat exchanger ($r = 75$ mm).

Previous work (Lu et al., 1996) shows that the shape of the advancement profiles highlights the main limiting phenomena: in the case of a strong thermal limitation, the reaction starts at the heat exchanger side, and a reactive front (called heat front) moves from this exchanger side through the reactive medium. On the other hand, if the limitation in the reaction process is predominantly due to mass transfer, a single reactive front, called the mass front, moves from the gas diffuser through the reactive medium during the reaction.

When variation of k is nonlinear, these extreme behaviors are combined, with preponderance of each of them at different global advancements according to values of X_S. In the typical case of Figure 4, the transformation is initially governed by the weak coupling between the two limitations: it leads to two progressive reactive fronts, heat front and mass front, respectively, from heat exchanger and gas diffuser. When the main limitation becomes strongly of mass transfer, as $k(x)$ drops, the change of behavior is evident on the three local profiles. On the advancement profiles, the heat front nearly stops and reaction evolves only from the gas diffuser side; while the local pressure drops towards the equilibrium pressure, mainly on the heat exchanger side where the reactive gas can no longer flow. Therefore, the available temperature drop (bounded by $T_{eq}[P(r)]$ and T_c) becomes very small. So, the range of values swept by local thermodynamic conditions T and P falls sharply during the reaction process when the coupling evolves towards a dominance in mass-transfer limitation. This change in the main phenomenon takes places at global advancements always clearly inferior to the value $X_{global} = X_S$ (for example, at $X_{global} = 0.3$ for $X_S = 0.5$).

These results emphasize that the temperature profile evolution reflects local information concerning the permeability pattern $k(x)$. Therefore, as this temperature profile is measurable, these observations are useful for the practical point of view.

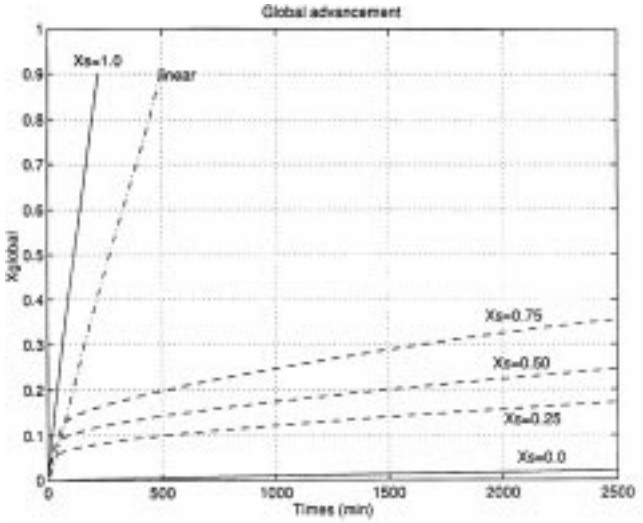

Figure 3. Influences of linear and nonlinear permeability evolutions on global advancement.

Simulations with: constant permeability $X_S = 0$, that is, $k_0 = 10^{-13}$ m^2, and $X_S = 1$, that is, $k_1 = 10^{-16}$ m^2 (solid lines); linear (dash-dotted line), and nonlinear (dash line) permeability evolutions between $k_0 = 10^{-13}$ m^2 and $k_1 = 10^{-16}$ m^2. (Synthesis $P_c = 0.5$ bar.)

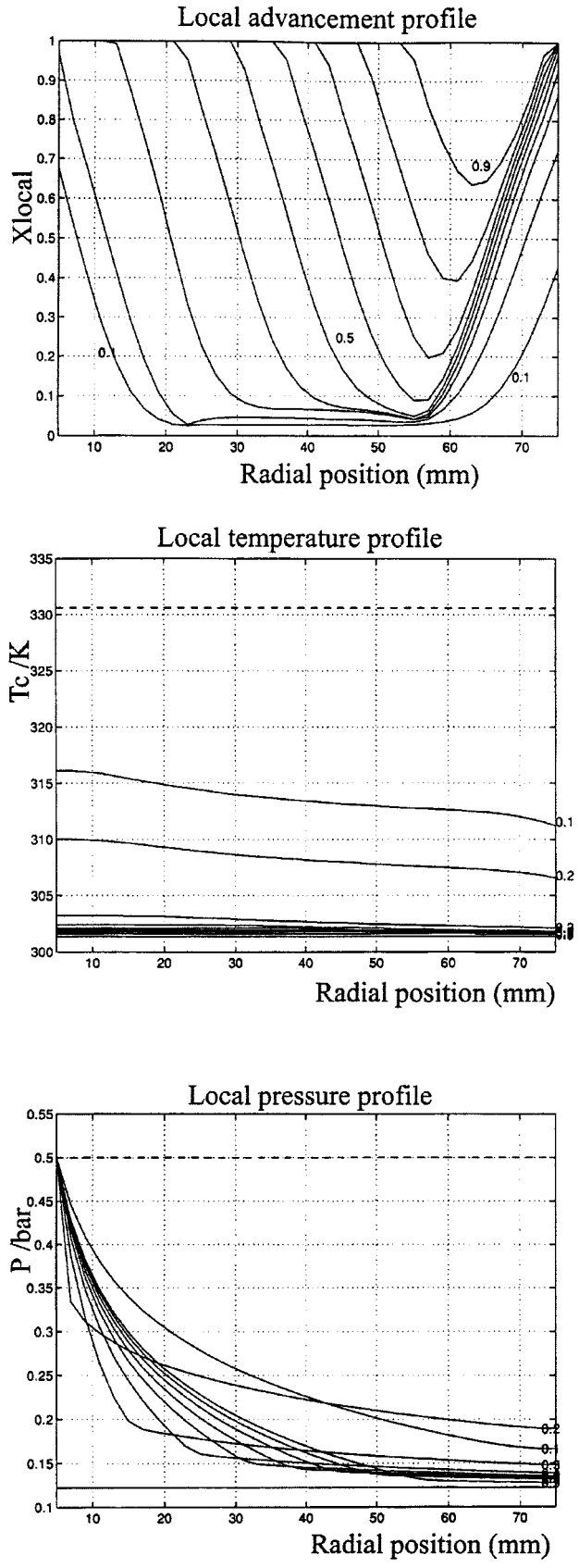

Figure 4. Simulations of local advancement, temperature and pressure profiles.

(Nonlinear evolutions of permeability, $X_S = 0.5$, $\alpha = 5$.)

Permeability Identification of Reactive Blocks

The objective is to identify the permeability of typical reactive blocks used in chemical heat transformers in order to validate the nonlinear evolution assumed in Eq. 9.

Experimental protocol

The reactor is a stainless steel cylinder (ID = 150 mm) with a coolant circuit and an electric heater on its periphery to release or supply heat of reaction (Figure 5). The inner hollow cylinder is a central gas diffuser which supplies the ammonia gas. The reactive block samples are 100 mm high. The anisotropic properties of this media lead to the assumption of one-dimensional heat and mass transfer along its radial direction. Experiments conducted by Prades (1992) in such a reactor have confirmed that the axial flux is negligible. The measurements include:

- Thermodynamic conditions imposed on the two boundaries of the reactive media, that is, P_C (from the gas diffuser) and T_C (from the heat exchanger)
- Global advancement of the reaction X
- Radial temperature profiles, by four thermocouples at different positions
- Pressures on the two extreme radial positions of the reactor

The uncertainties are in the following ranges: thermocouple measurement ± 1°C; global advancement measurements $\pm 2.5\%$; λ and h_{sw} estimations $\pm 15\%$ and $\pm 20\%$, respectively.

The reaction involved in IMPEX blocks is the synthesis and decomposition of hexaammoniacate $Mn(NH_3)_6Cl_2$, that is

$$Mn(NH_3)_2Cl_2 + 4NH_3 \Leftrightarrow Mn(NH_3)_6Cl_2 + 4\Delta H$$

This reaction has been extensively studied at the laboratory

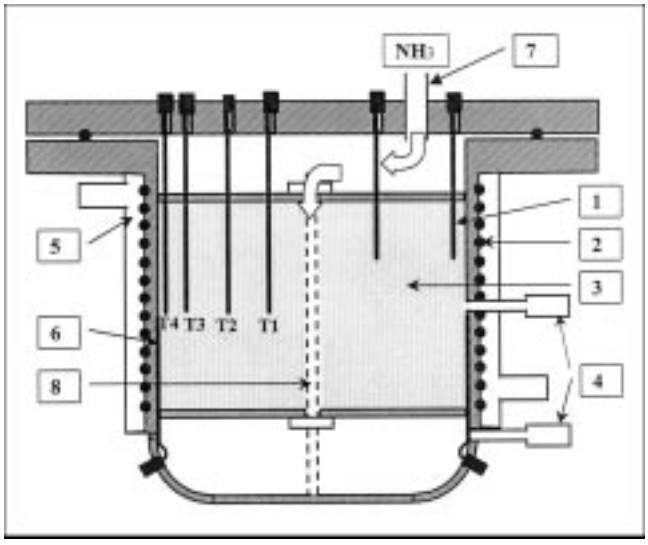

Figure 5. Reactor and its probes.

(a) Thermocouples T1 to T6; (2) electric heater; (3) reactive media; (4) pressure gauge; (5) annular heat exchanger (coolant); (6) thermocouple at the wall; (7) gas inlet; (8) gas diffuser.

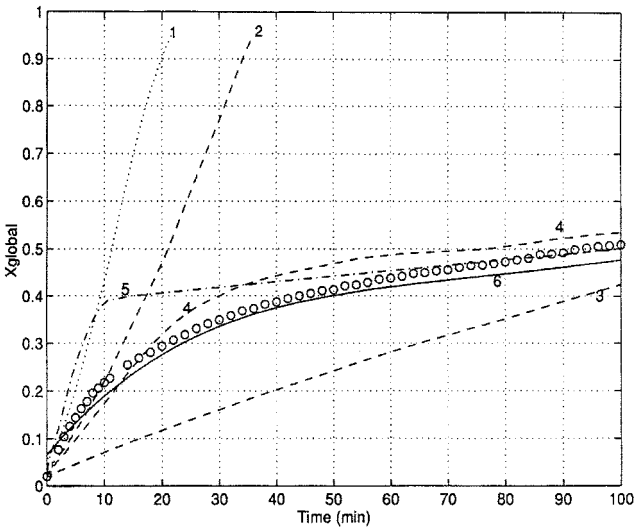

Figure 6. Global advancement: Experimental vs. simulation results for constant and different linear and nonlinear evolutions of permeability.

(Synthesis, $P_c = 0.3$ bar).

Experiment	Simulations
oooooooo	*Constant permeability*
	$k = \infty$ $k = 10^{-13}$ m^2 $k = 10^{-14}$ m^2
	Dot...1. Dash--2 Dash--3
	Linear permeability
	$k_0 = 710^{-14}$ m^2 $k_1 = 10^{-18}$ m^2
	Dash--------4
	Nonlinear
	($k_0 = 5\times10^{-13}$ m^2, $k_1 = 10^{-16}$ m^2)
	$X_S = 0.3$ $X_S = 0.1$
	Dash-dot.-.-.-5 Solid line____6

(Marty, 1991; Goetz and Marty, 1993), particularly for its equilibrium and reaction kinetics.

Experiments have been carried out according to the following protocol:

- Initially, the block temperature is uniformly maintained at T_C, therefore, the pressure is P_{eq} (T_C)
- At $t = 0$, the evaporator is connected to the reactor, and imposes an input pressure P_C to the reactor
- At $t > 0$, the reaction goes on under local conditions P, T, that evolve between the equilibrium conditions and the constraints P_C, T_C (see Figure 1).

The main physical parameters used for simulations are thermal conductivity, heat-transfer coefficient at the heat exchanger wall, and permeability. Obviously, the change in block texture during reaction influences these three parameters. As IMPEX blocks studied are of high conductivity, the conduction in the media is not a limiting phenomenon and its variation has little influence on the transformation of the media. Therefore, the conductivity is considered to evolve linearly in the reaction process. On the other hand, the heat transfer at the wall, represented by h_{SW}(see Eqs. 7 and 8) is an influencing phenomenon. So, its variation between the two ends h_{SW0} and h_{SW1} must be taken into account and discussed (see the subsection on the influence of heat-transfer coefficient at the heat exchanger wall). For the permeability, the previous nonlinear permeability evolution is assumed (Eq. 9).

Evolution of the permeability during the experimental reaction process

The interest of presenting this IMPEX A is its significant slowdown of the reaction that it undergoes during experimental operating conditions of low pressure. Its characteristics are presented in Table 1. Figure 6 shows the comparison of measured global advancement (Prades, 1992) with that obtained by simulation using different evolution of permeability values: constant, linear, and nonlinear (Eq. 9). Figure 7 shows the corresponding temperatures evolution, that is, measured values at four radial positions and simulated ones only at two outskirts positions r_1 and r_4. For reasons of clarity, simulated temperature profiles with constant permeability (corresponding to plots No. 2 and No. 3, Figure 6) have not been presented in Figure 7.

Figures 6 and 7 clearly show that, when mass transfer is correctly simulated, in other words, if a nonlinear permeability evolution like Eq. 9 has been integrated in the model, the global advancement and local temperature profiles can be simultaneously simulated in a satisfactory manner.

In Figure 6, the simulation, based on a linear evolution of k (plot 4), gives a global advancement which could be considered to be quasi-satisfactory for this IMPEX A. However, this simulation outlines two problems:

- First, this situation could only be realized when k_1 is extremely low, that is, $k = k_1 = 10^{-18}$ m^2. This value is not realistic at all: according to the parameter sensitivity study made by Lu et al. (1996), the reaction in such a porous media is completely blocked when k is as low as 10^{-16} m^2.

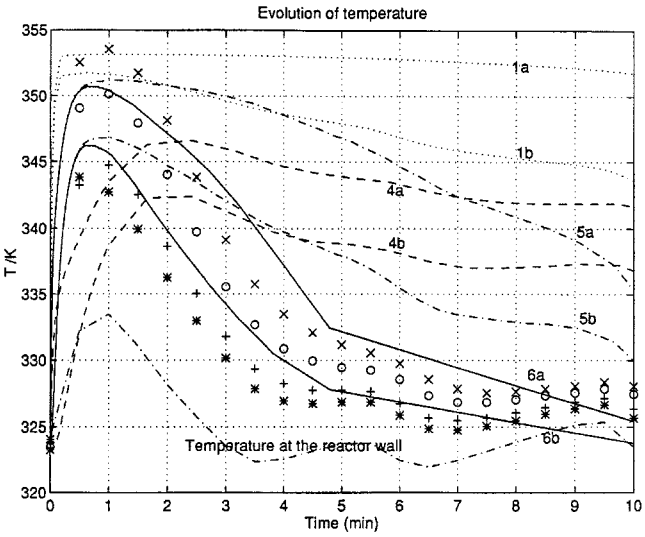

Figure 7. Temperature evolutions in the reactor: experimental vs. simulation results in the same conditions as Figure 6.

(Synthesis, $P_c = 1.3$ bar.) Experimental temperatures at positions: T1—'x'; T2—'o'; T3—'+'; T4—'*'. Simulations for cases 1, 4, 5, and 6 of Figure 6. Suffix *a* and *b* correspond to positions T1 and T4.

• Secondly, a considerable discrepancy is observed between the calculated temperature and measured ones (Figure 7, plot 4). This discrepancy, more significant in the beginning of the reaction (15°C in the first 7 min), can be explained by an inappropriate simulation of permeability evolution.

The comparison of Figures 6 and 7 indicates a rapid and classical evolution of temperatures toward $T_{eq}(P_c) = 355$ K (20°C during the first 3 min) initially. Then, the global reaction rate decreases significantly, thus, local temperatures must tend toward an equilibrium value. Figure 7 shows, however, that experimental temperatures are far away from the equilibrium temperature corresponding to the input pressure P_C. This indicates that the local pressure is far away from P_C, and follows an evolution with a rapid decrease, similar to measured temperature evolution; therefore, the corresponding equilibrium temperature is close to the local temperature. This type of pressure evolution in the reaction process could be induced only by a significant evolution of permeability.

It should be noted that an increase of h_{SW} in the reaction process will cause a temperature drop towards a value closer to that of the reactor wall, hence, a better fitting of experimental temperatures. However, this higher h_{SW} will lead to an increase of reaction rate, hence, a worse fitting of the experimental global advancement. Therefore, adjusting the heat-transfer coefficient h_{SW} is not an adequate solution.

This experimental behavior of both global advancement and local temperatures could only be simulated by utilizing a permeability function $k(x)$, which represents a sharp drop from $x = 0$ to 1. Therefore, the transformation of IMPEX A is correctly simulated by using Eq. 9, with the identified value of $X_S = 0.1$. This typical example has shown that it is necessary to pay particular attention to the heat- and mass-transfer parameters modeling when the structure of the material changes during the reaction.

Permeability Evolution According to Reactant Density

In this part, a new series of IMPEX reactive blocks is studied. They present the same graphite density, but with an increasing salt ratio. Their characteristics are listed in Table 1 (IMPEX B, C, D). Comparing with the previous IMPEX A, this new series of IMPEX shows remarkable contact heat-transfer coefficients at the reactor wall (up to 3,000 W/m$^2\cdot$K). Experiments have been carried out at low pressure of 0.2 bar (with an equilibrium drop of 20°C, Figure 8), and at high pressure of 2 bars (with an equilibrium drop of 40°C, Figures 9 and 10). The operating conditions have been listed in Table 2. The objective is to identify the main parameters characterizing the permeability (k_0, k_1 and X_S), and their evolution vs. the block density.

Order of magnitude of permeability

First, the permeability is assumed constant during the reaction. Experimental results at high pressure lead to the permeability order of magnitude related to the IMPEX salt ratio: the range is from 10^{-12} to 10^{-14} m^2. So, a diminution of permeability by a factor of 100 seems to be reached when the salt ratio increases from 40% to 63%. These results also demonstate that simulation which ignores the limitation created by mass transfer could be acceptable for IMPEX B (40% of salt). However, IMPEX C and D, which have a higher salt ratio, present an evident limitation to their transformation due to the transfer of reactive gas (even at a pressure as high as 2 bar), whereas their total porosity is still significant (from 40 to 52%, respectively, for IMPEX C and D).

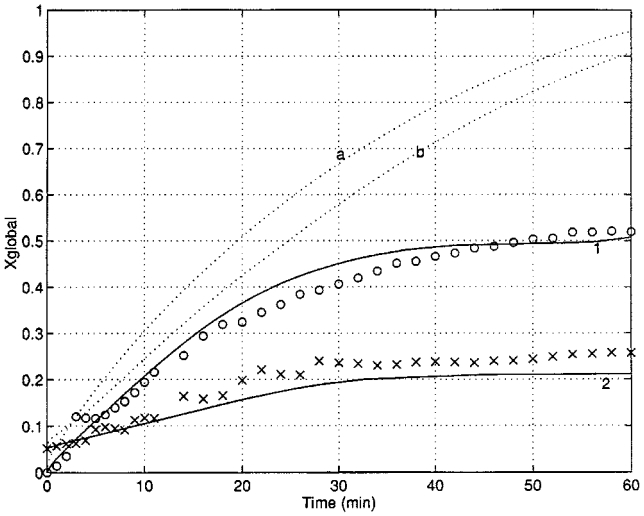

Figure 8. Identification, at low pressure, of permeabilities for different IMPEX.

Global advancement (Synthesis, $P_c = 0.2$ bar).

	IMPEX B	IMPEX C
Experiment	Symbol ooooo	Symbol xxxxx
Simulation with $k = \infty$	Dotted line ...a...	Dotted line ...b...
Simulation with nonlinear evolution of k: k_0, k_1, and X_S	$k_0 = 4\times10^{-12}$ $k_1 = 10^{-16}$ $X_S = 0.35$, solid line 1	$k_0 = 10^{-12}$ $k_1 = 10^{-16}$ $X_S = 0.3$ solid line 2

Transformation of IMPEX at low pressure

An accurate identification of the set of parameters (k_0, k_1 and X_S) characterizing the permeability require experimental data obtained in operating conditions leading to a more severe mass-transfer limitation, particularly for IMPEX B and C. Experimental results on these IMPEX, at a low pressure of 0.2 bar, provide means to identify these parameters. As such a material presents excellent heat-transfer characteristics (see Table 1), the main limitation clearly comes from mass transfer, and the plot shape of the global advancement exhibits a typical slowdown effect (Figure 8).

Permeability parameters used in Eq. 9 have been identified for IMPEX B and C (see their values in Figure 8's caption). They lead to a very good representation of the significant slowdown effect on the global advancement of the reaction (Figure 8) and the corresponding temperature profiles.

Transformation of IMPEX at high pressure

In order to validate the previous identifications, the same permeability parameters are used to re-simulate the same blocks B and C reacting at high pressure of 2 bar. Figures 9 and 10 present a comparison between experimental and sim-

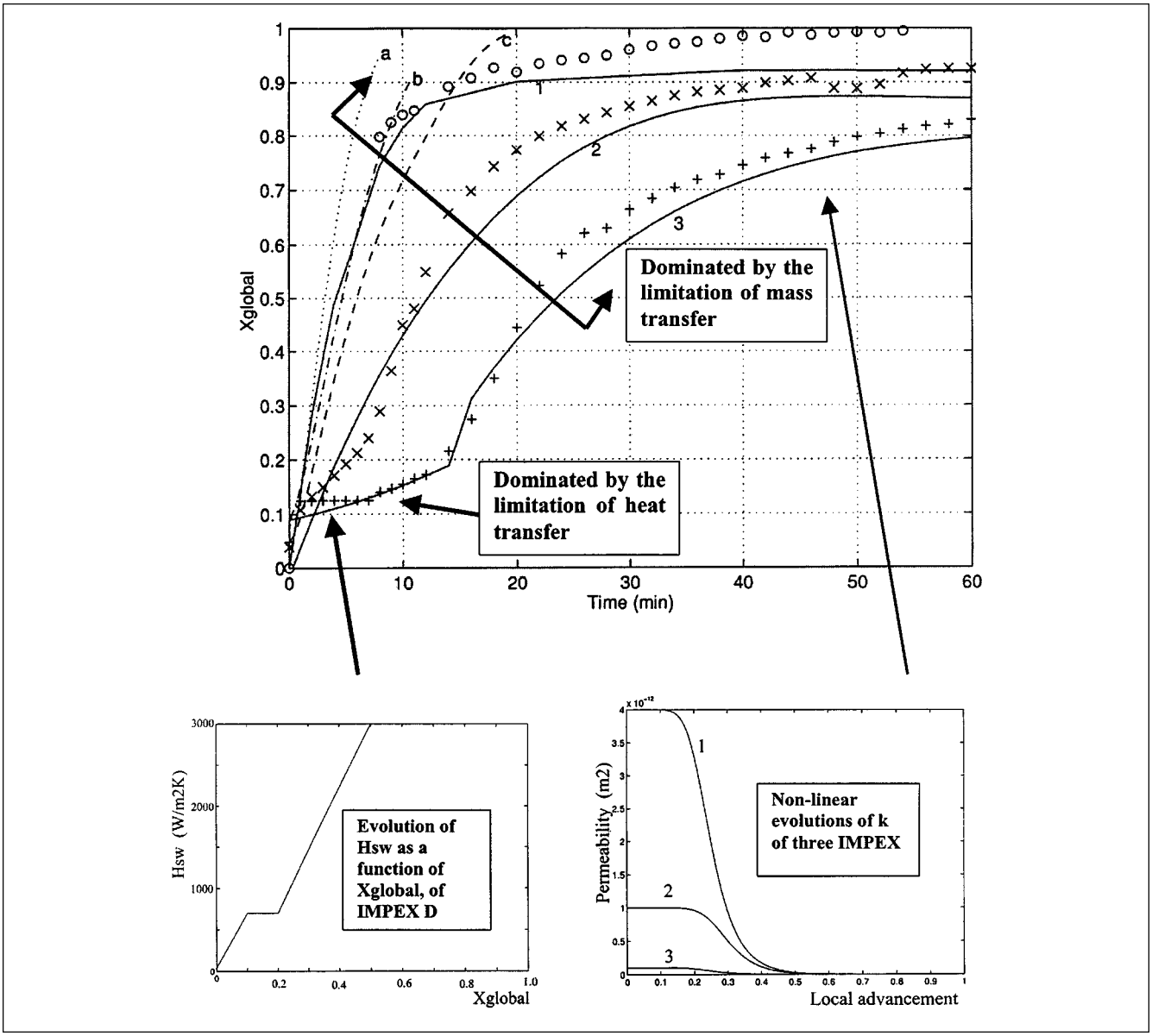

Figure 9. Simulations of global advancement at high pressure for different IMPEX using permeabilities identified at low pressure for IMPEX B and C, and at high pressure for IMPEX D.

(Synthesis, $P_c = 2$ bar.)

	IMPEX B	IMPEX C	IMPEX D
Experiment	Symbol oooo	Symbol xxxx	Symbol + + + +
Simulation with $k = \infty$	Dotted line ....a....	Dotted line ...b....	Dotted line ....c....
Simultion with nonlinear evolution of k: k_0, k_1 and X_S	$k_0 = 4 \times 10^{-12}$, $k_1 = 10^{-16}$ and $X_S = 0.35$, solid line 1	$k_0 = 10^{-12}$, $k_1 = 10^{-16}$ and $X_S = 0.3$, solid line 2	$k_0 = 5 \times 10^{-13}$, $k_1 = 10^{-16}$ and $X_S = 0.25$, solid line 3

ulated results. They show a rather good agreement for both global advancements and local profiles which validates Eq. 9 of the permeability behavior. Yet, IMPEX C shows some difference around $t = 10$ mn, mainly due to the estimation of h_{SW}. This point will be widely discussed later.

In addition, the nonlinear evolution of IMPEX D permeability has been identified in the same operating conditions (see Figure 9's caption). The fit between calculated and measured values is very satisfactory for both temperature and advancement of the reaction (Figures 9 and 10).

The identified values of k_0, k_1 and X_S for IMPEX B, C, and D enable to quantify the diminution of permeability with the block density. For salt ratio from 40% to 63%, the initial permeability k_0 is reduced by an order of 10, while k_1 remains constant at a value of about 10^{-16} m^2, the value of X_S is in a relatively weak range from 0.35 to 0.25, but has a strong influence on the slowdown of the reaction rate. So, this parameter X_S seems to be a very sensitive and important one.

These results reflect only a tendency of the observed evolution from the available experiments. It will be useful to re-

IMPEXB

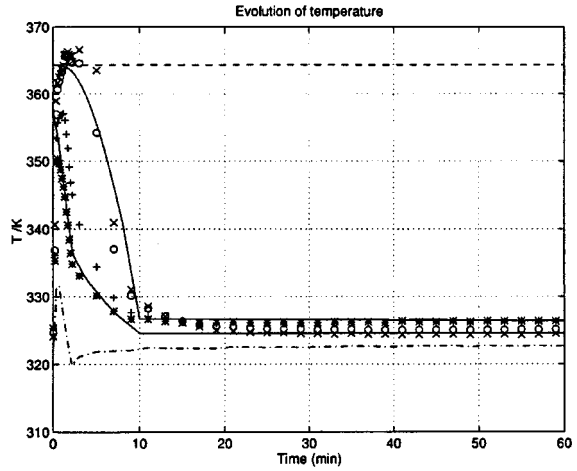

IMPEX C

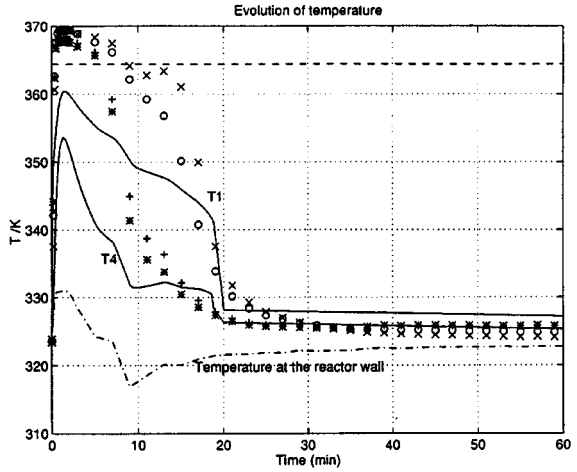

IMPEX D

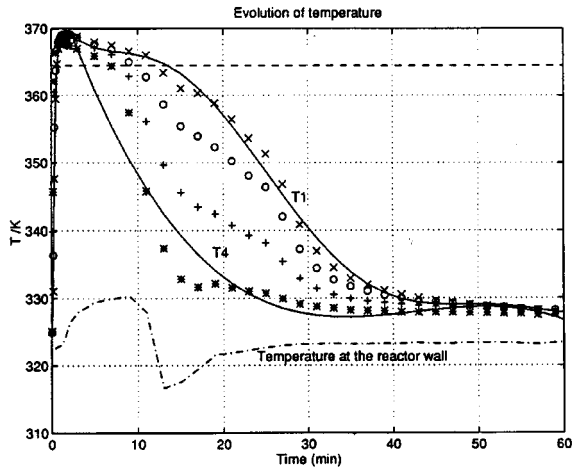

Figure 10. Simulations of temperature evolutions in the same conditions as Figure 9.

Experimental temperatures at positions: T1—'*x*'; T2—'*o*'; T3—'+'; T4—'∗.'

Table 2. Experimental Values of Thermodynamical Operating Conditions for IMPEX B, C, D

Operating Pressure in Synthesis Equilibrium drop $\Delta T_{eq} = T_C - T_{eq}(P_C)$		$P_{CS} = 2$ bar $\Delta T_{eq} = 40°$	$P_{CS} = 0.2$ bar $\Delta T_{eq} = 20°$
Synthesis	$T_{eq}(P_{CS})$	364.4	311.5
	T_{CS}	324.4	294.5
	$P_{eq}(T_{CS})$	0.38	0.07
Decomposition	$T_{eq}(P_{CD})$	378.5	329.9
	T_{CD}	418.5	349.9
	$P_{eq}(T_{CD})$	8.78	0.56

fine them by means of more precise measurements (particularly for pressure profiles within the reactive block) for a wider range of IMPEX (according to the salt ratio and graphite binder density) and for various operating conditions (P_C).

Influence of heat-transfer coefficient at the heat exchanger wall

In some experiments, global advancements exhibit a delay at the onset of the reaction. This is especially observed for IMPEX D at 2 bar (Figure 9). This particular evolution is linked to a very low heat-transfer coefficient h_{SW0} at the beginning of the synthesis, which can only be improved when the transformation of the peripheral part of the reactive block leads to an increase of the block stress and therefore a better contact with the reactor wall. Hence, the heat-tranfer coefficient reaches its highest value h_{SW1}.

This variation of h_{SW} is less important for IMPEX B and C, because a less significant expansion of block is expected in the reaction process, corresponding to their lower salt ratio. Moreover, during the reactions of these materials (IMPEX B and C) that have a higher initial permeability value (k_0), the necessary time interval that the reactive block needs to expand and, thus, to have a satisfactory contact with the wall, is greatly reduced than that of IMPEX D. So, the evolution of h_{SW} does not have a noticeable influence on the global transformation of IMPEX B and C.

Therefore, a linear evolution of h_{SW} between h_{SW0} and h_{SW1} has been used for IMPEX B and C. However, for IMPEX D, it is necessary to fine-tune the representation of the h_{SW} evolution. So, an additional identification has been carried out: the shape of h_{SW} vs. X_{global} is represented in a small plot (Figure 9). Actually, a very weak initial value of h_{SW0} ($h_{SW0} = 40$ W/m^{2}K (see Table 1)) leads to a significant heat-transfer limitation in the beginning of the reaction (see the plateau around $X_{\text{global}} = 0.15$, Figure 9). It should be noted that, for IMPEX C, a double identification (k and h_{SW}) could also be carried out, as its advancement curve shows the evidence of heat-transfer limitation during the first 8 min. Such a fine-tuned heat-transfer parameter fitting is not the objective of this study; a linear evolution of h_{SW} has therefore been kept. This has led to a slightly poorer representation of the global advancement and the local temperatures during the first few minutes.

It appears that for materials having relatively high salt ratio and, therefore, an important variation of their physical characteristics during the reaction on process, there exist two

limitations: first, heat-transfer limitation which is particularly strong at the onset of the reaction, and secondly, mass-transfer limitation which is demonstrated at a later stage of the reaction.

Conclusions

In this article, the importance of mass transfer in the process of reversible solid gas reaction within porous reactive media has been analyzed and discussed in detail. The material used is a high performance reactive one (IMPEX), which has excellent heat- and mass-transfer qualities and high energetic densities. By analyzing and experimenting its performances under extremely unfavorable mass-transfer conditions (such as low pressure), we have brought to light the special characteristics of the evolution of mass-transfer parameters that will be of practical interest for all porous reactive material working under such conditions.

A parameter sensitivity study has demonstrated the nonlinear permeability evolution during the reaction process as observed in the simulations of global advancement and local profiles of advancement, temperature, and pressure. This nonlinear evolution is confirmed by numerous experiments. The general model integrated with the nonlinear permeability evolution is a very useful tool for identification of parameters relative to mass transfer for reactive materials at low pressure, and could consequently predict the performances of IMPEX blocks at all pressure levels. The results from this study have practical applications in the design of optimal reactor configuration (Mazet and Lu, 1998) and to avoid such reactor performance drop down.

On the other hand, experimental measurements of mass-transfer parameters at the onset and at the end of the reaction are in progress. Difficulties of dynamic measurements of such parameters actually lead to use the global modeling, coupled with chemical kinetics, heat transfer, and mass transfer to determine these values. When direct measurements of permeability are available, an additional validation of the conclusions presented in this article will be expected.

Acknowledgment

The authors gratefully acknowledge the EEC support (Contract Joule2 JOU2 CT 94-0445). The authors also greatly appreciate the help of Prof. B. Jean (INRS Energy, Montreal).

Notation

$C_p(x)$ = specific heat capacity of media in the function of x, J/m^3·K
I = source term, mol/(m^3·s)
k = permeability of the reactive block, m^2
t = time, s
$x(r)$ = local advancement
X_{global} = global advancement
ϵ = porosity
λ_e = equivalent medium thermal conductivity, W/m·K
ρ = apparent density of graphite binder, kg/m^3
μ = gas viscosity, kg/m·s
ΔH = reaction enthalpy, J/mol of gas

Subscripts

0 = in the beginning of synthesis reaction
1 = at the end of synthesis reaction
c = imposed value
e = equivalent
eq = equilibrium value
p = pellet
w = reactor wall

Literature Cited

Castaing-Lasvignottes, J., and B. Spinner, ''Transformation of Solid-Gas Reactors for Thermochemical Processes. Influence of Transfers Parameters or Anisotropic Fixed Beds and Heat Exchanger Performances,'' *Proc. München Discuss. Meeting, Heat Transfer Enhancement by Additives*, Session IV, 12 (Oct. 10–11, 1994).

Coste, C., G. Crozat, and S. Mauran, ''Procédé de Mise en Oeuvre de Réactions Gaz-Solide,'' French Patent No. 83 09 885 (June 15, 1983); Extension U.S. Patent No. 4,595,774 (June 17, 1986).

Goetz, V., and A. Marty, ''A Model for Reversible Solid-Gas Reactors Submitted to Temperature and Pressure Constraints: Simulation of the Rate of Reaction in Solid-Gas Reactor Used as Chemical Heat Pump,'' *Chem. Eng. Sci.*, **47**, 4445 (1993).

Guilleminot, J. J., ''Heat and Mass Transfer Characteristics of Composites for Adsorption Heat Pumps,'' *Int. Absorption Heat Pump Conf.*, **AES-Vol. 31**, 401 (1993).

Lu, H. B., N. Mazet, and B. Spinner, ''Modelling of Gas-Solid Reaction—Coupling of Heat and Mass Transfer with Chemical Reaction,'' *Chem. Eng. Sci.*, **51**(15), 3829 (1996).

Marty, A., ''Etude par Microcalorimétrie de la Reactivité de Deux Ammoniacates de Chlorure de Manganèse,'' *J. of Thermal Analysis*, **37**, 479 (1991).

Mauran, S., M. Lebrun, P. Prades, M. Moreau, B. Spinner, and C. Drapier, ''Composite Actif et Procédé de Mise en Oeuvre de Processus Physico-Chimique, Gaz Solide, ou Gaz Liquide Utilisant comme Milieu Réactionnnel un Tel Composite Actif,'' French Patent No. FR 91 0303 (Apr. 11, 1991).

Mauran, S., P. Prades, and F. L'Haridon, ''Heat and Mass Transfer in Consolidated Reacting Beds for Thermochemical Systems,'' *Heat Recovery Systems and CHP*, **13**, 315 (1993).

Mauran, S., N. Mazet, and J. L. OMS, ''Productions de Froid à Basse Température (−20 à−40°C) par Pompes à Chaleur Chimiques Solide-Gaz: Problématiques des Transferts dans les Milieux Poreux Réactifs,'' *IXVIII Congrés Int. du Froid*, Montreal (Aug. 10–17, 1991).

Mazet, N., M. Amouroux, and B. Spinner, ''Analysis and Experimental Study of the Transformation of a Non-Isothermal Solid-Gas Reacting Media,'' *Chem. Eng. Commun.*, **99**, 155 (1991).

Mazet, N., and H. B. Lu, ''Improving the Performance of Reactor under Unfavorable Operating Conditions of Low Pressure,'' *Appl. Thermal Eng. J.*, **18**, 819 (1998).

Prades, P., ''Transferts Thermiques en Milieu Poreux Composite: Caractérisation et Développement de Reactifs Consolidés Pour Transformateur Thermochimique Solide-Gaz,'' PhD Thesis, Univ. de Perpignan, France (1992).

Satzger, P., F. Ziegler, D. Stitou, B. Spinner, and G. Alefeld, ''Advanced Sorption Chillers for Gas Cooling,'' *Absorption Heat Pumps and Refrigeration Systems*, ASHRAE Symp. Ser. (Feb. 17–21, 1996).

Spinner, B., ''Pompes à Chaleur Basées sur la Réaction Renversable Entre un Gaz et un Solide ou une Solution Saturée: Recherche et Développement,'' *Récents Progrès en Génie des Procédés*, Lavoisier Ed. (1988).

Spinner, B., ''Ammonia-Based Thermochemical Transformers,'' *J. Heat Recovery Sys. and CHP*, **13**, 301 (1993).

Spinner, B., ''Changes in Research and Development of Objectives for Closed Solid-Sorption Systems, Key Note Paper,'' *Proc. Int. Absorption Conf.*, Montreal (Sept. 17–20, 1996).

Sun, L. M., and F. Meunier, ''Non-Isothermal Adsorption in a Bidisperse Adsorbent Pellet,'' *Chem. Eng. Sci.*, **42**, 2899 (1987).

Szekely, J., J. W. Evans, and H. Y. Sohn, *Gas-Solid Reaction*, Academic Press, New York (1976).

Wojtanowicz, A. K., ''Experimental Determination of Formation Damage Pore Blocking Mechanisms,'' *J. of Energy Res. Technol*, ASME, **110**, 34 (1988).

Manuscript received Dec. 16, 1996, and revision received June 7, 1999.